Science Advances
AAAS

Supplementary Materials for

lncRNA-GM targets Foxo1 to promote T cell–mediated autoimmunity

Yali Chen *et al.*

Corresponding author: Kun Chen, kunchen@cams.cn; Xuetao Cao, caoxt@immunol.org

Sci. Adv. **8**, eabn9181 (2022)
DOI: 10.1126/sciadv.abn9181

This PDF file includes:

Supplementary Materials and Methods
Figs. S1 to S9
Original data

Supplementary Materials and Methods

Antibodies, recombinant cytokines, and reagents

The following reagents and antibodies were used: for surface staining, anti-CD19 (1D3, eBioscience), anti-CD3 (145-2C11, Biolegend), anti-CD4 (RM4-5, Biolegend), anti-CD8α (53-6.7, Biolegend), anti-CD25 (PC61, Biolegend), anti-CD44 (IM7, Biolegend), anti-CD62L (MEL-14, Biolegend), anti-Ly-6C (HK1.4, Biolegend), anti-Ly-6G (1A8, Biolegend), anti-CD11b (M1/70, Biolegend), anti-B220 (RA3-6B2, Biolegend); for intracellular staining, anti-IL17A (TC11-18H10, BD), anti-IL4 (11B11, Biolegend), anti-IFNγ (XMG1.2; eBioscience), anti-Foxp3 (150D/E4, eBioscience). For mouse T cell stimulation, anti-CD3 (145-2C11) and anti-CD28 (37.51) were from BD; recombinant mouse IL-2 (402-ML), IL-6 (406-ML), IL-4 (404-ML), IL-12 (419-ML), IL-1β (401-ML), IL-23 (1887-ML) and recombinant human TGF-β1 (7754-BH) were from R&D Systems; neutralizing anti-mouse IFN-γ (XMG1.2) was from Biolegend and anti-mouse IL-4 (11B11) was from BioXcell. For human T cell stimulation, recombinant human IL-4, IL-12, IL-6, IL-1β, and IL-23 were from PeproTech; neutralizing anti-human IFN-γ (B27), anti-human IL-4 (MP4-25D2) were from Biolegend; Anti-human CD3 (UCHT1) and CD28 (CD28.2) were from Biolegend. mTOR inhibitor Rapamycin (Beyotime Biotech), mTOR activator MHY1485 (MedChemExpress), H3K9Ac inhibitor CPI-637 (Selleck), Foxo1 inhibitor AS1842856 (MedChemExpress) were used for T cell treatment.

In vitro T cell differentiation

For mouse T cell differentiation, mouse $CD4^+$ T cells were purified from total splenocytes using positive selection (Miltenyi, $CD4^+$ T Cell Isolation Kit), with purity of $CD4^+$ T cells > 95%. The purified $CD4^+$ T cells were stimulated with 5 μg/ml anti-mouse CD3 and 2 μg/ml anti-mouse CD28, and supplemented with a series of cytokines for T cell subsets differentiation as followed, 20 ng/ml IL-12 and 10 μg/ml anti-IL4 for Th1 differentiation; 20 ng/ml IL-4 and 10 μg/ml anti-IFNγ for Th2 differentiation; 30 ng/ml IL-6, 3 ng/ml h-TGF-β1, 10 ng/ml IL-1β, 20 ng/ml IL-23, 10 μg/ml anti-IFNγ and 10 μg/ml anti-IL4 for optimal pathogenic Th17 differentiation; 30 ng/ml IL-6, 3 ng/ml h-TGF-β1, 10 μg/ml anti-IFNγ and 10 μg/ml anti-IL4 for non-pathogenic Th17 differentiation; 30 ng/ml IL-6, 10 ng/ml IL-1β, 20 ng/ml IL-23, 10 μg/ml anti-IFNγ and 10 μg/ml anti-IL4 for pathogenic Th17 differentiation; 10 ng/ml IL-2, 10 ng/ml h-TGF-β1, 10 μg/ml anti-IFNγ and 10 μg/ml anti-IL4 for iTreg differentiation. After 3-day stimulation, cells were collected for later analysis.

For human T cell differentiation, human $CD4^+$ T cell subsets were collected from human peripheral blood PBMC, and then were stimulated with 5 μg/ml anti-human CD3 and 2 μg/ml anti-human CD28, and a series of cytokines for T cell subsets differentiation as followed, 20 ng/ml h-IL-12 and 10 μg/ml anti-human IL4 for Th1 differentiation; 20 ng/ml h-IL-4 and 10 μg/ml anti-human IFNγ for Th2 differentiation; 20 ng/ml h-IL-6, 3 ng/ml h-TGF-β1, 10 ng/ml h-IL-1β, 20 ng/ml h-IL-23, 10 μg/ml anti-human IFNγ and 10 μg/ml anti-human IL4 for Th17 differentiation; 100 U/ml h-IL-2, 10 ng/ml h-TGF-β1, 10 μg/ml anti-human IFNγ and 10 μg/ml anti-human IL4

for iTreg differentiation.

Real-time quantitative PCR

Cells were collected at indicated times for RNA extraction. Total RNA was extracted with TRIzol reagent according to the manufacturer's methods. cDNA was synthetized from total RNA with Reverse Transcriptase M-MLV (RNase H-) Kit (Takara). Real-time quantitative PCR was analyzed by QuantStudio 6 or 7 Flex (Thermo, Applied Biosystems) using Premix Ex Taq II Kit (Takara). Cycle thresholds (CT) of different samples were normalized to β-Actin for mRNA or to U6 for lncRNA respectively.

The primers used for qPCR as following, *mlncRNA-GM*, forward: TGC CAT AAC AGA GTC TGG AAC TC, reverse: AGA AAG GTA GGA ACT GTC CAG CC; *mIl17*, forward: CTC AAA GCT CAG CGT GTC CAA ACA, reverse: TAT CAG GGT CTT CAT TGC GGT GGA; *mIl17f*, forward: CAG GAA GAC AGC ACC ATG AA, reverse: TCT TCT CCA ACC TGA AGG AAT TAG; *mRORc*, forward: AGG CCA TTC AGT ATG TGG TGG AGT, reverse: TGT GTG GTT GTT GGC ATT GTA GGC; *mIl23r*, forward: CAC TGC CGA CCA AGG AAT CT, reverse: GCA TGA GGT TCC GAA AAG CC; *mTbx21*, forward: CTT GGA TCC TTC GCC TAC CC, reverse: CTT CCC AGA CAC CTC CAA CC; *mFoxo1*, forward: GAA GAG GCT CAC CCT GTC G, reverse: CCT CCC TCT GGA TTG AGC AT; *mFoxp3*, forward: GCG AAA GTG GCA GAG AGG TA, reverse: GAG GAG CTG CTG AGA TGT GA; *mIl10rb*, forward: CTT CTG GTG CCA GCT CTA GG, reverse: GAA GTC GCA

CTG AGT CGA GG; *mGpr83*, forward: CGC CCT TCA CTT TGG TCA TC, reverse: CAGAGGGAGCGCACAATGTC; *mHaus3*, forward: TGC CAG TTG TAA AGG GCG AT, reverse: ACC AAA CTC TCT AGT TGC CGA; *mMxd4*, forward: TCG GTC AGG ACT CAA GTT GC, reverse: CGG ATC CTG CCG AGA TTT GT; *mGstm1*, forward: ATA CTG GGA TAC TGG AAC GTC C, reverse: AGT CAG GGT TGT AAC AGA GCA T; *mIfna4*, forward: TGA TGA GCT ACT ACT GGT CAG C, reverse: GAT CTC TTA GCA CAA GGA TGG C; *mIfnb1*, forward: TAC ACT GCC TTT GCC ATC CA; reverse: AGT TGA GGA CAT CTC CCA CG; *hAK026392.1* (*h-lncRNA-GM*), forward: AAC CTC CCA CTG CTC CCT GTC, reverse: GGC TCT GTT CTG CTT CTG TCT GC; *hIL17*, forward: GAG GAC AAG AAC TTC CCC CG, reverse: CTC TCA GGG TCC TCA TTG CG; *hBATF*, forward: GAA AAC CAG CGC GTT TCC AT, reverse: GCA GCC CAA GTT CCT ACA CT; *hIL17F*, forward: GAA AAC CAG CGC GTT TCC AT, reverse: GCA GCC CAA GTT CCT ACA CT; *hIL23R*, forward: GCC TGG CTC TGA AGT GGA AT, reverse: CCT CCA TGA CAC CAG CTG AA; *hIL21*, forward: TTG CTT CTT AGT TAC TCA CGG T, reverse: TGT CCA ACT GCA AGT TAG ATC CT; *hFOXP3*, forward: GGC CAC ATT TCA TGC ACC AG, reverse: GCT CCC TGG ACA CCC ATT C; *hIL10*, forward: GCT CTT GCA AAA CCA AAC CA, reverse: TCT CGA AGC ATG TTA GGC AGG; *hIL10RA*, forward: GTC TTG GCT CAG ACG CTC AT, reverse: CAG GGT CTG GCT ACA GTT GG; *hIL10RB*, forward: CCT TGC TGT GGT GCG TTT AC, reverse: TTG CCG CTC TCA GAG TCT TC.

FIGURES AND FIGURE LEGENDS

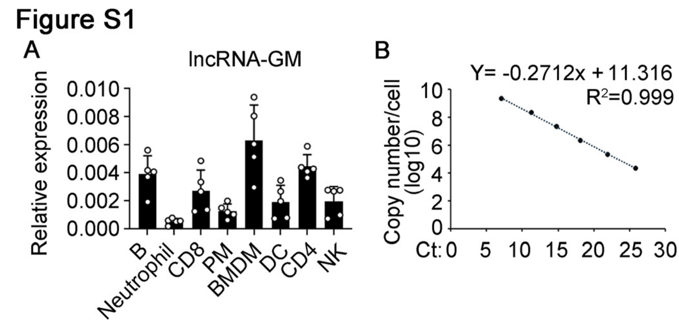

Fig. S1. lncRNA-GM expression in immune cells.

(**A**) qPCR analysis of lncRNA-GM mRNA expression in different immune cells (n=5). (**B**) The standard curve of copy numbers derived from plasmid DNA absolute expression measured by qPCR. Results are presented as mean ± SD (**A**). One representative experiment of three is shown. PM, peritoneal macrophages; BMDM, bone marrow-derived macrophages; DC, dendritic cells; NK, natural killer cells.

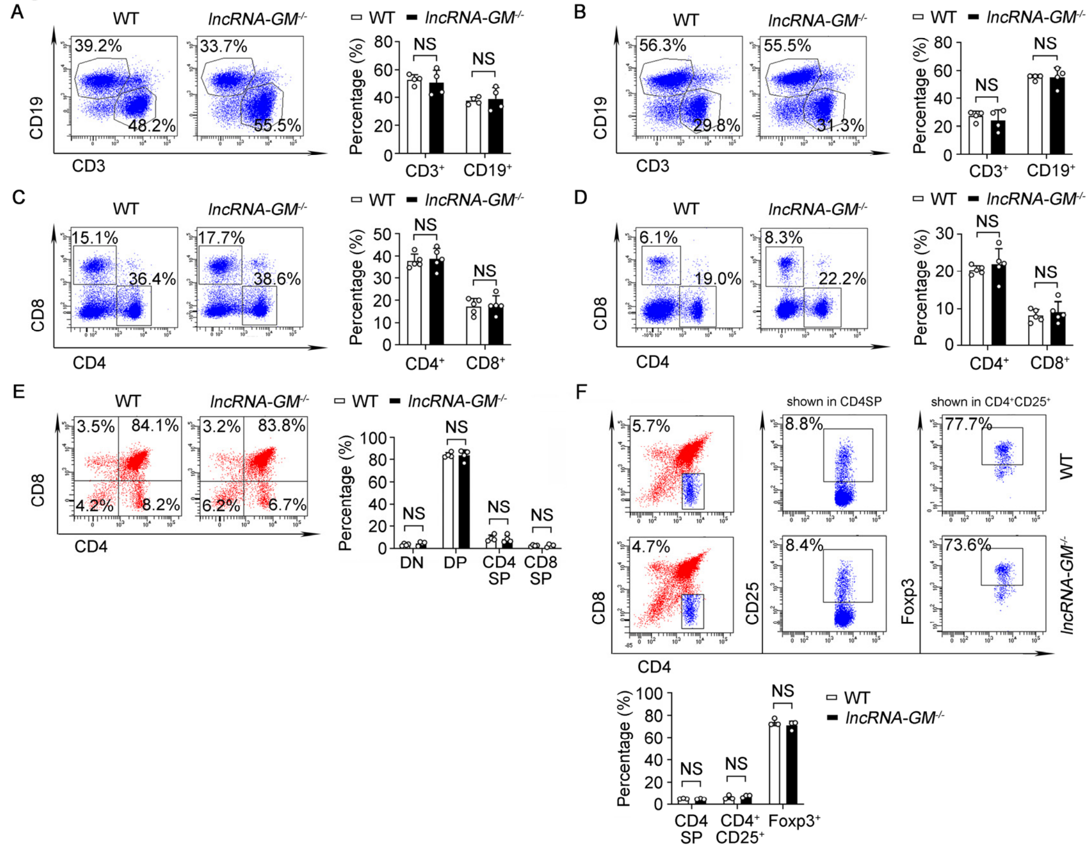

Fig. S2. lncRNA-GM does not affect the development of T cells.

(**A** and **B**) Flow cytometric analysis of $CD3^+$, $CD19^+$ cells in lymph node (**A**) and spleen (**B**) from wide-type (WT) and *lncRNA-GM*$^{-/-}$ mice (n=4). (**C** and **D**) Flow cytometric analysis of $CD4^+$ and $CD8^+$ cells in lymph node (**C**) and spleen (**D**) (n=5). (**E**) Flow cytometric analysis of T cells in thymus (n=4). (**F**) Flow cytometric analysis and quantification of nTreg ($CD4^+$ $CD25^+$ $Foxp3^+$) thymocytes (n=3). Results are presented as mean ± SD (**A** to **F**). One representative experiment of three is shown. NS, not significant.

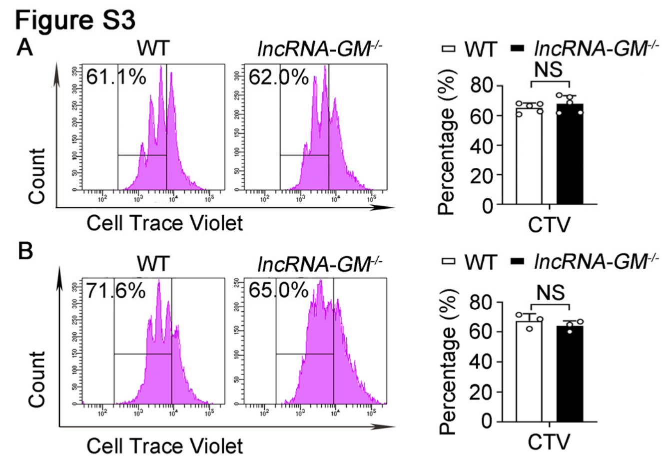

Fig. S3. lncRNA-GM does not affect the proliferation of T cells.

(**A** and **B**) $CD4^+$ (**A**) and $CD8^+$ (**B**) T cells proliferation after treatment with anti-CD3 (5 μg/ml) and anti-CD28 (2 μg/ml) 3 days (n=3 to 5). Results are presented as mean ± SD (**A** and **B**). One representative experiment of three is shown. NS, not significant.

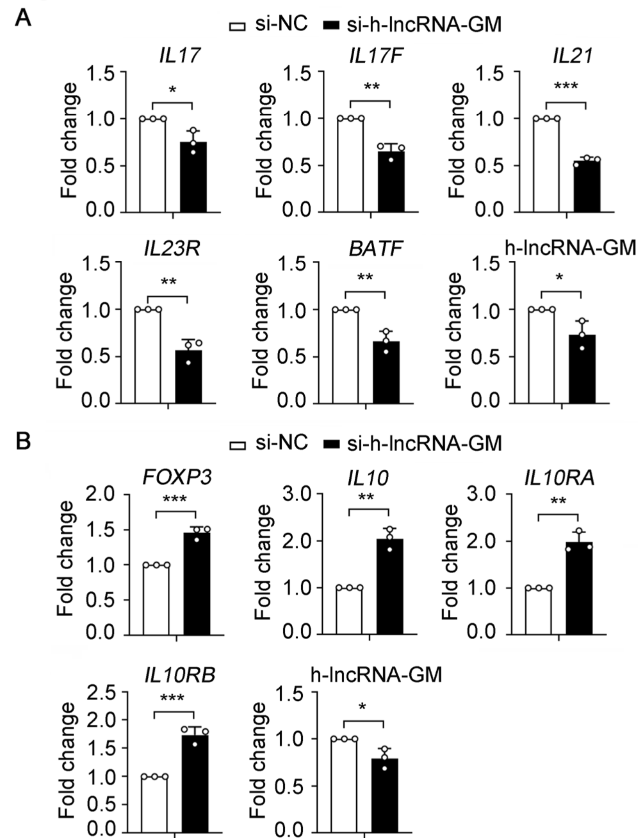

Fig. S4. Silencing of human *lncRNA-GM* inhibits Th17-related gene expression and promotes Treg-related gene expression.

(**A**) qPCR analysis of *IL17*, *IL17F*, *IL21*, *IL23R* and *BATF* mRNA expression in human Th17 cells (n=3). (**B**) qPCR analysis of *FOXP3*, *IL10*, *IL10RA* and *IL10RB* mRNA expression in human Treg cells (n=3). Results are presented as mean ± SD (**A** and **B**). $^{*}P < 0.05$; $^{**}P < 0.01$; $^{***}P < 0.001$.

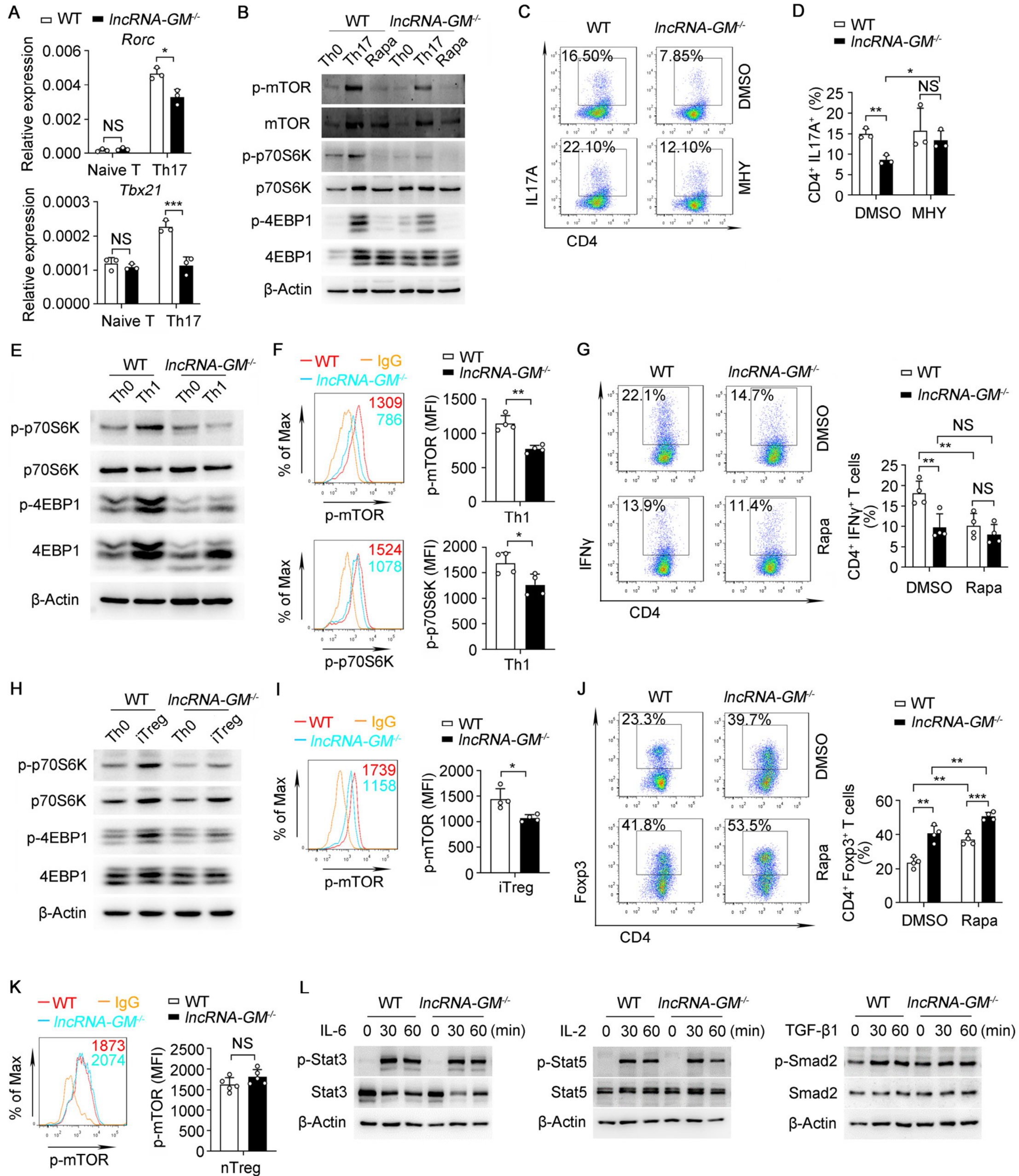

Fig. S5. lncRNA-GM promotes Th1/Th17 cell and inhibits iTreg cell development by enhancing mTORC1 signaling.

(**A**) qPCR analysis of *Rorc* and *Tbx21* mRNA expression in naïve T and Th17 cells (n=3). (**B**) Immunoblot analysis of mTOR and downstream signaling pathway in WT and *lncRNA-GM*$^{-/-}$ Th17 cells after treatment with DMSO or 50 nM Rapamycin (Rapa). (**C** and **D**) Flow cytometric analysis (**C**) and quantification (**D**) of IL17A^{+}

cells in WT and *lncRNA-GM*$^{-/-}$ Th17 cells after treatment with DMSO and 10 μM MHY1485 (MHY) (n=3). (**E**) Immunoblot analysis of mTOR downstream signaling pathway in WT and *lncRNA-GM*$^{-/-}$ Th0 (α-CD3/CD28) and Th1 cells cultured for 3 days. (**F**) Phosphorylation of mTOR and p70S6K was measured by flow cytometry from WT and *lncRNA-GM*$^{-/-}$ Th1 cells (n= 4). (**G**) Flow cytometric analysis and quantification of IFNγ^{+} cells in WT and *lncRNA-GM*$^{-/-}$ Th1 cells after treatment with DMSO and 200 nM rapamycin (Rapa) (n=4). (**H**) Immunoblot analysis of mTOR downstream signaling in WT and *lncRNA-GM*$^{-/-}$ iTreg cells. (**I**) Phosphorylation of mTOR was measured by flow cytometry from WT and *lncRNA-GM*$^{-/-}$ iTreg cells (n= 4). (**J**) Flow cytometric analysis and quantification of Foxp3^{+} cells in iTreg cells after treatment with DMSO and 50 nM rapamycin (Rapa) (n=4). (**K**) Phosphorylation of mTOR was measured by flow cytometry from nTreg (CD4^{+} CD25^{+}) thymocytes stimulated with anti-CD3 (5 μg/ml), anti-CD28 (2 μg/ml) and rIL-2 (10 ng/ml) 3 days (n=5). (**L**) Immunoblot analysis of indicated protein levels in naïve CD4^{+} T cells after treatment with 30 ng/ml IL-6 (left), 10 ng/ml IL-2 (middle) and 10 ng/ml TGF-β1 (right). Naive CD4^{+} T cells were cultured *in vitro* under optimal pathogenic Th17 cell polarizing conditions for 3 days. Results are presented as mean ± SD (**A**, **D**, **F**, **G**, **I**, **J** and **K**). One representative experiment of three is shown. *P < 0.05; **P < 0.01; ***P < 0.001; NS, not significant.

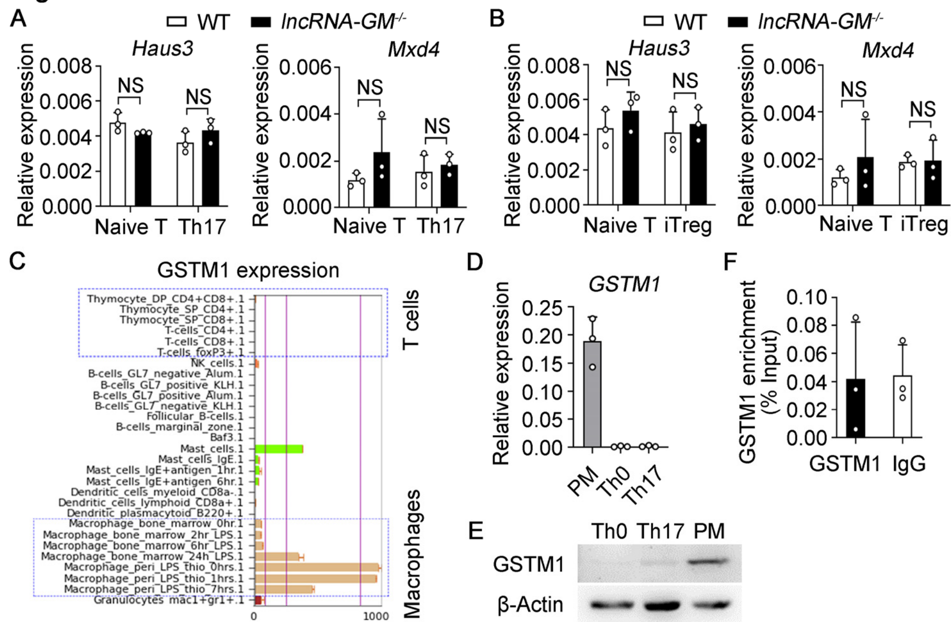

Fig. S6. lncRNA-GM promotes Th17 cell differentiation independent of *in cis* function and GSTM1.

(**A** and **B**) qPCR analysis of *Haus3* and *Mxd4* mRNA expression in Th17 (**A**) or iTreg (**B**) cells from WT and *lncRNA-GM*$^{-/-}$ mice (n=3). (**C**) Analysis of GSTM1 expression in different immune cells at BioGPS website. (**D** and **E**) qPCR (**D**) and immunoblot (**E**) analysis of GSTM1 expression in macrophages and T cells (n=3). (**F**) RIP-qPCR analysis of lncRNA-GM immunoprecipitated by GSTM1 antibody in Th17 cells (n=3). Results are presented as mean ± SD (**A**, **B**, **D** and **F**). One representative experiment of three is shown. NS, not significant.

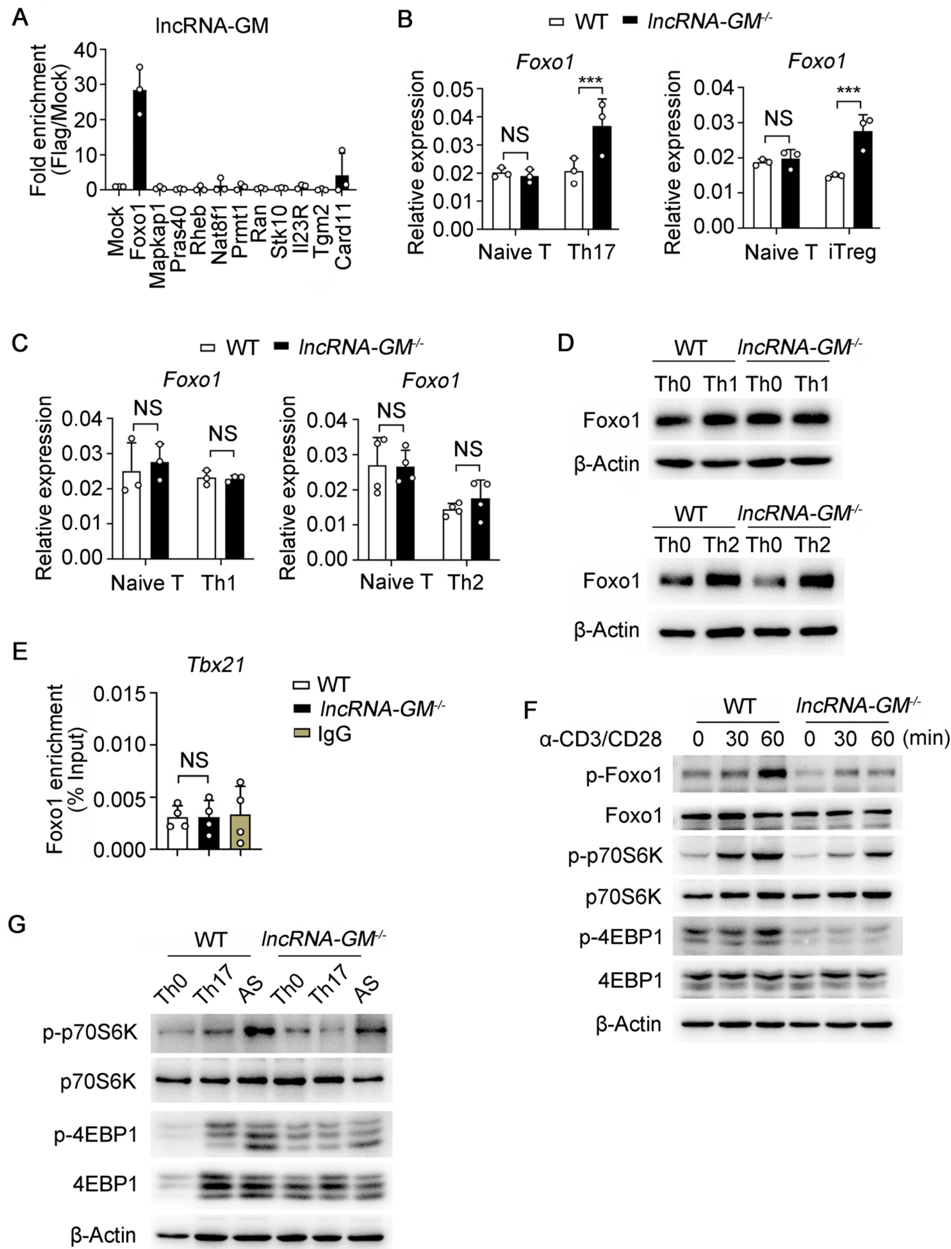

Fig. S7. lncRNA-GM directly binds to Foxo1 and reduces Foxo1 expression.

(**A**) RIP-qPCR analysis of lncRNA-GM immunoprecipitated by Flag antibody in HEK293T cells transfected with indicated plasmids (n=3). (**B**) qPCR analysis of *Foxo1* mRNA expression in Th17 (left) or iTreg (right) cells (n=3). (**C** and **D**) qPCR (**C**) and immunoblot (**D**) analysis of Foxo1 levels in WT and *lncRNA-GM*$^{-/-}$ Th1 and Th2 cells (n=3 to 4). (**E**) ChIP-qPCR analysis the recruitment of Foxo1 to *Tbx21*

promoter regions in Th1 cells (n=4). (**F**) Immunoblot analysis of p-Foxo1 (Ser256), p-p70S6K (Thr421/Ser424) and p-4EBP1 (Thr37/46) levels in naïve $CD4^+$ T cells after treatment with anti-CD3 (5 μg/ml) and anti-CD28 (2 μg/ml) for indicated minutes. (**G**) Immunoblot analysis of mTOR downstream signaling pathway in WT and *lncRNA-GM*$^{-/-}$ Th17 cells after treatment with DMSO or AS1842856 (AS). Naive $CD4^+$ T cells were cultured *in vitro* under optimal pathogenic Th17 cell polarizing conditions for 3 days. Results are presented as mean ± SD (**A**, **B**, **C** and **E**). One representative experiment of three is shown. ***$P < 0.001$; NS, not significant.

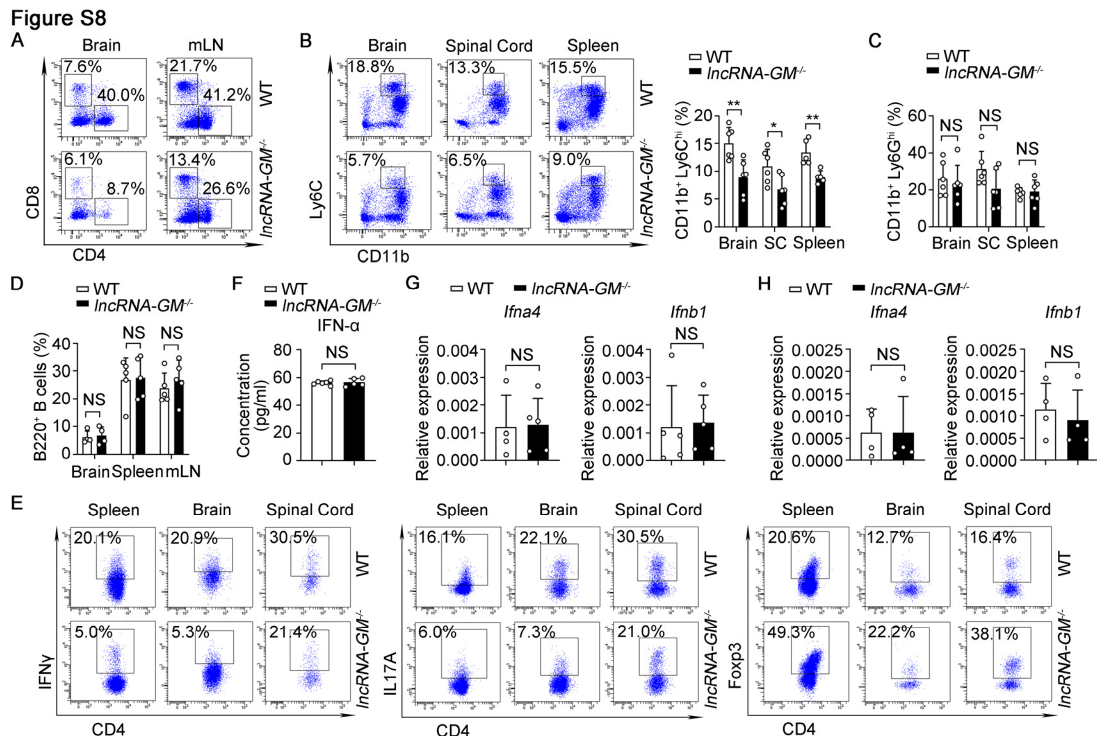

Fig. S8. *lncRNA-GM* deficiency reduces inflammatory cell infiltration during EAE development, independently of type I IFN production.

(**A**) Flow cytometric analysis of $CD4^+$ and $CD8^+$ T cells within total $CD45^{hi}$ cells in brain and mesenteric lymph node (mLN) from WT and *lncRNA-GM*$^{-/-}$ mice with EAE. (**B**) Flow cytometric analysis and quantification of monocytes ($CD11b^+$ $Ly6C^{hi}$) within total $CD45^{hi}$ cells in spleen, brain and spinal cord (SC) (n=5 to 6). (**C** and **D**) Quantification of neutrophils ($CD11b^+$ $Ly6G^{hi}$) within total $CD45^{hi}$ cells in brain, spleen and SC (**C**), and quantification of B cells ($B220^+$) within total $CD45^{hi}$ cells in brain, spleen and mLN (**D**) (n=4 to 6). (**E**) Flow cytometric analysis of $IFN\gamma^+$ (left), $IL17A^+$ (middle) and $Foxp3^+$ (right) cells within total $CD45^{hi}$ cells in spleen, brain and spinal cord. (**F**) ELISA detection of sera IFN-α from WT and *lncRNA-GM*$^{-/-}$ mice with EAE (n=5 to 6). (**G** and **H**) qPCR analysis of *Ifna4* and *Ifnb1* mRNA expression in brain (**G**) and mLN (**H**) from WT and *lncRNA-GM*$^{-/-}$ mice (n=4 to 5). Results are

presented as mean ± SD (**B**, **C**, **D**, **F**, **G** and **H**). One representative experiment of three is shown. *P < 0.05; **P < 0.01; NS, not significant.

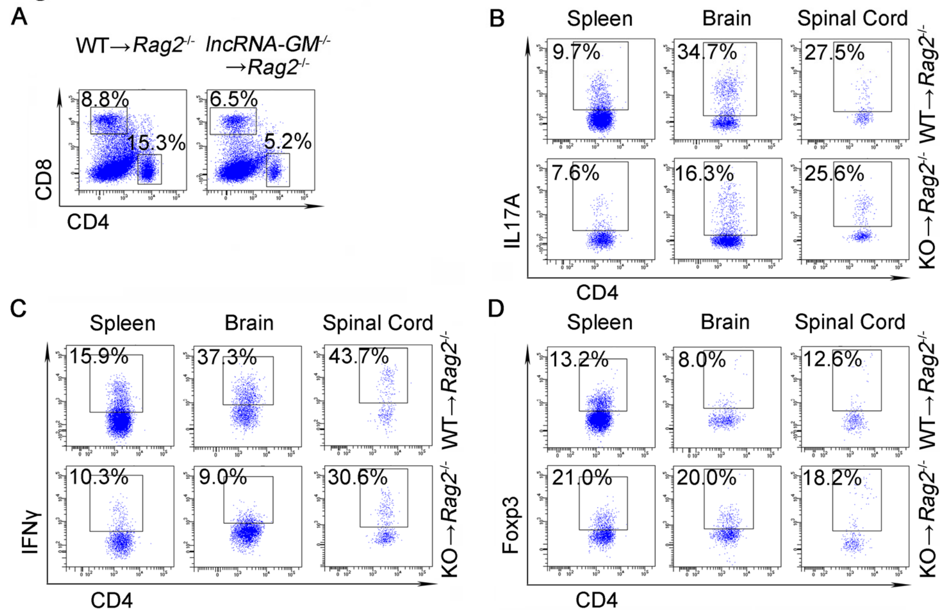

Fig. S9. Deficiency of *lncRNA-GM* reduces Th17 cell infiltration but promotes Treg cell infiltration during EAE by T cell adoptive transfer.

(**A**) Flow cytometric analysis of $CD4^+$ T and $CD8^+$ T cells in spleen from *Rag2*$^{-/-}$ recipients of WT and *lncRNA-GM*$^{-/-}$ (KO) mice. (**B** to **D**) Flow cytometric analysis of $IL17A^+$ (**B**), $IFN\gamma^+$ (**C**) and $Foxp3^+$ (**D**) cells within total $CD45^{hi}$ cells in spleen, brain and spinal cord from *Rag2*$^{-/-}$ recipients. One representative experiment of three is shown.

Original Data

Fig. 3G

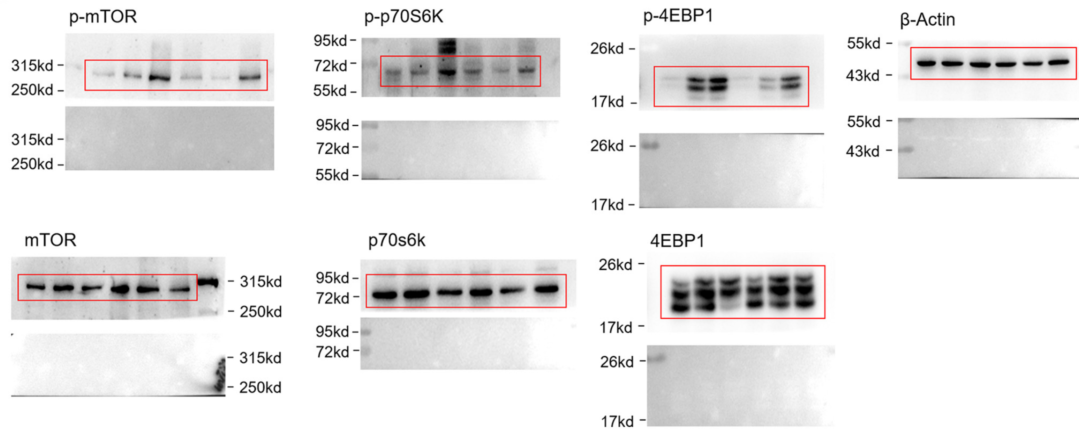

Fig. 4D

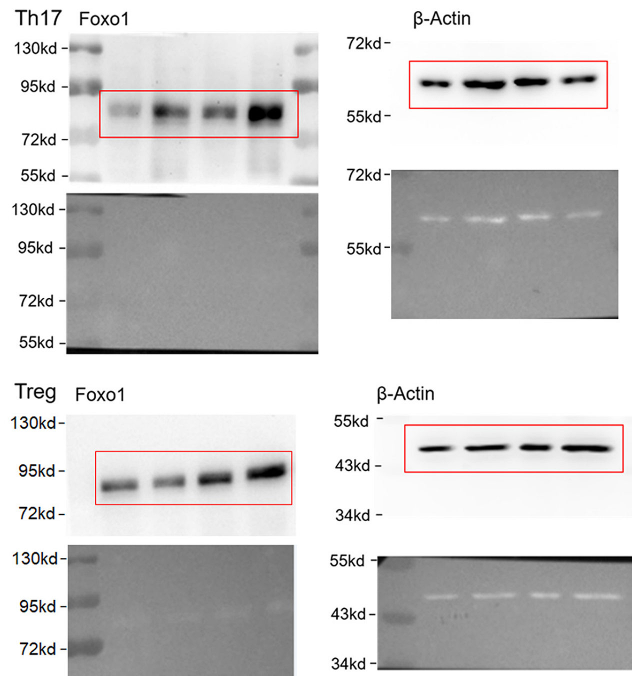

Fig.4H

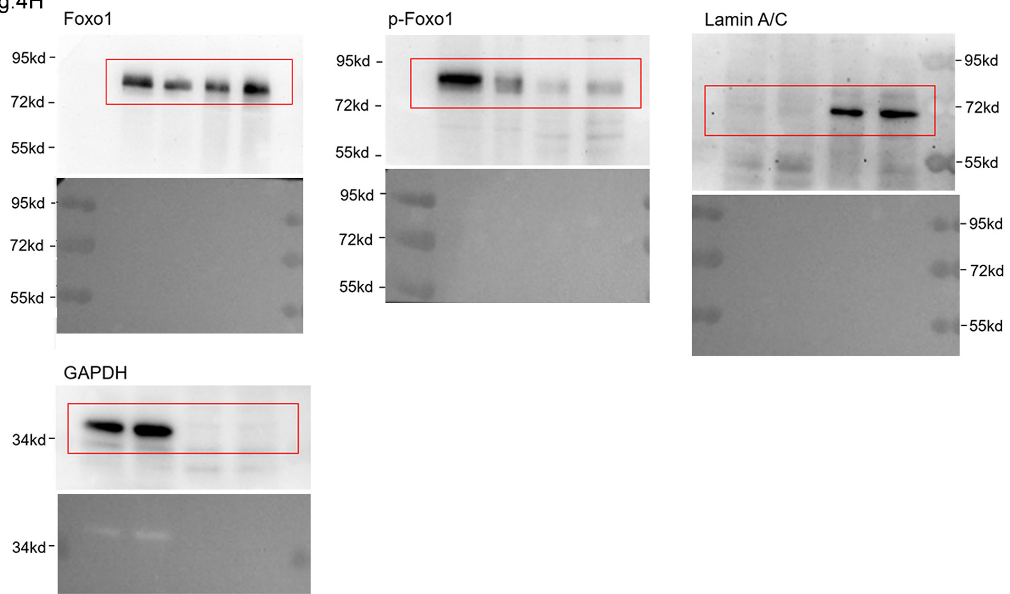

Fig.4J

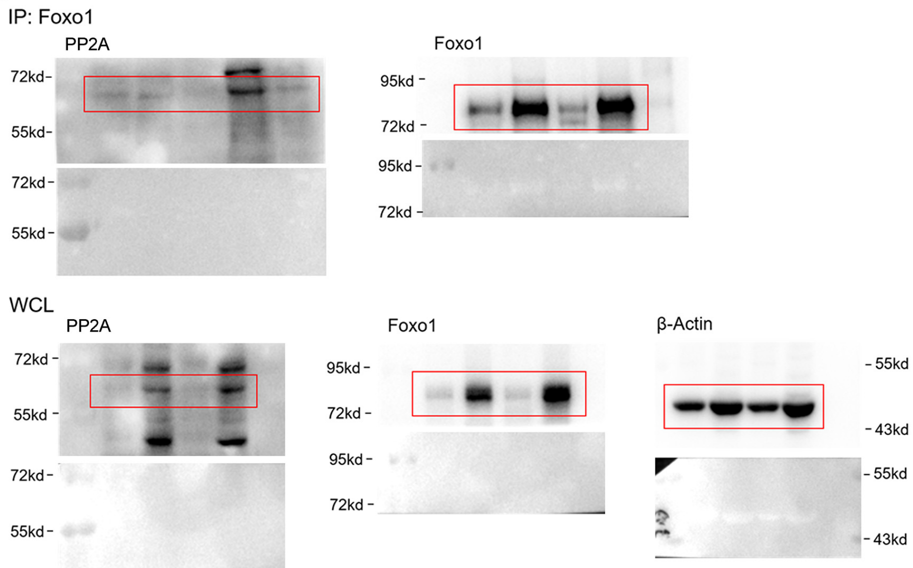

fig. S5B

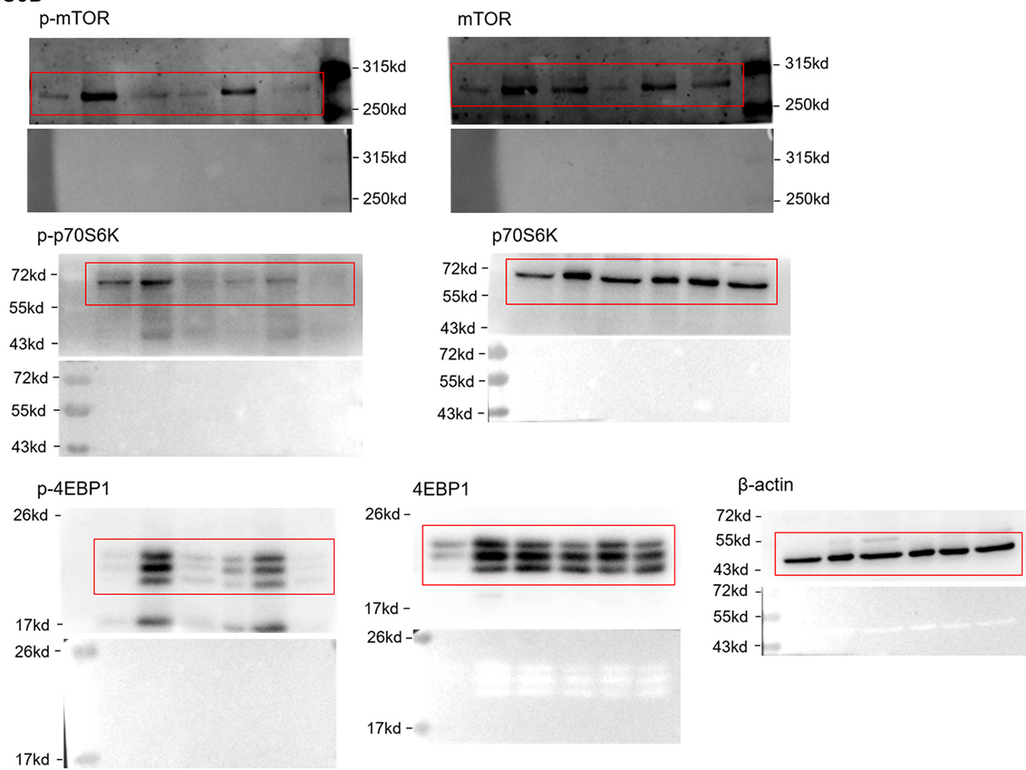

fig.S5E

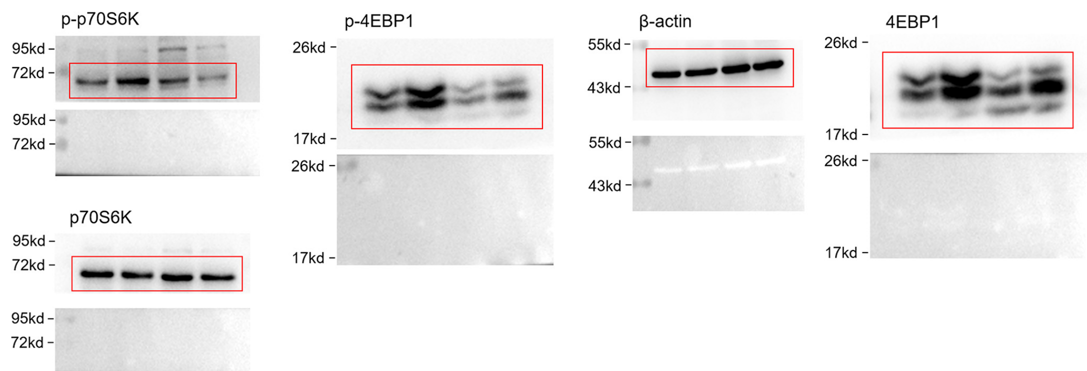

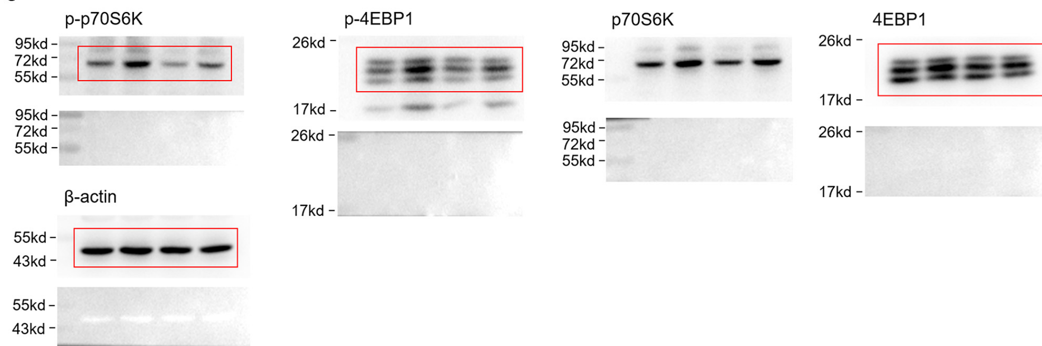
fig. S5H
p-p70S6K
95kd
72kd
55kd
95kd
72kd
55kd
β-actin
55kd
43kd
55kd
43kd
p-4EBP1
26kd
17kd
26kd
17kd
p70S6K
95kd
72kd
55kd
95kd
72kd
55kd
4EBP1
26kd
17kd
26kd
17kd

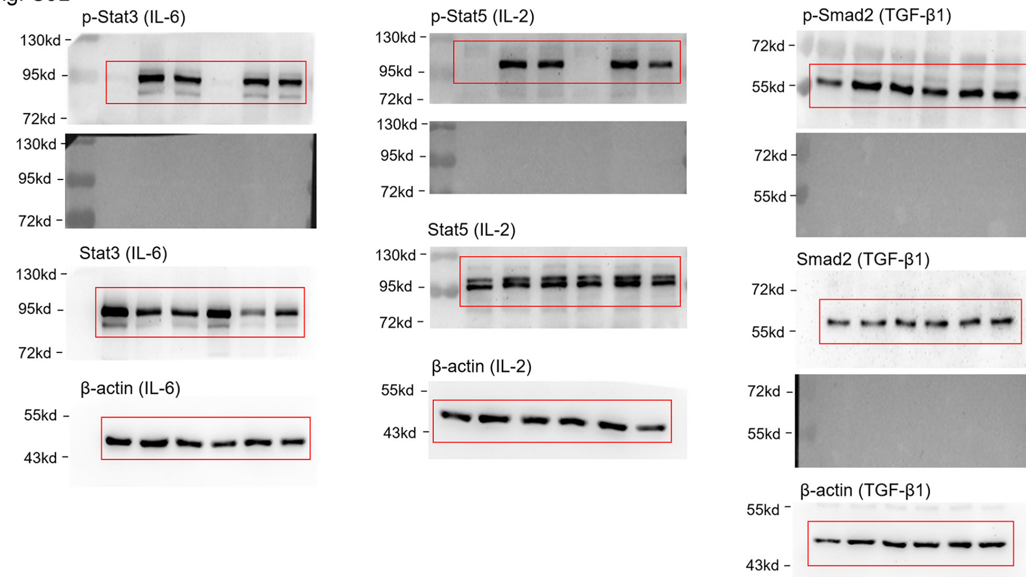
fig. S5L
p-Stat3 (IL-6)
130kd
95kd
72kd
130kd
95kd
72kd
Stat3 (IL-6)
130kd
95kd
72kd
β-actin (IL-6)
55kd
43kd
p-Stat5 (IL-2)
130kd
95kd
72kd
130kd
95kd
72kd
Stat5 (IL-2)
130kd
95kd
72kd
β-actin (IL-2)
55kd
43kd
p-Smad2 (TGF-β1)
72kd
55kd
72kd
55kd
Smad2 (TGF-β1)
72kd
55kd
72kd
55kd
β-actin (TGF-β1)
55kd
43kd

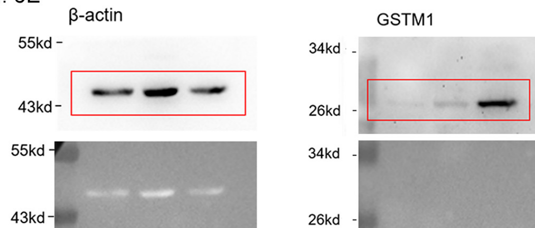
fig. 6E
β-actin
55kd
43kd
55kd
43kd
GSTM1
34kd
26kd
34kd
26kd

fig. S7D

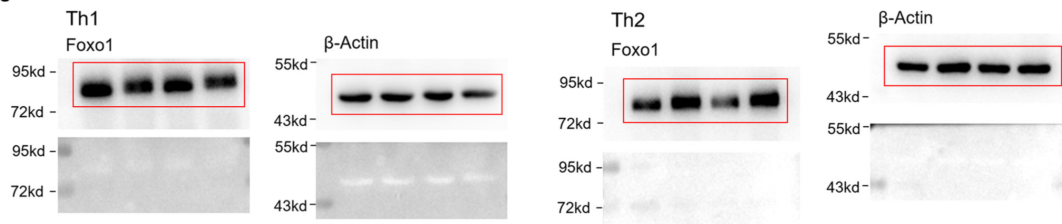

fig. S7F

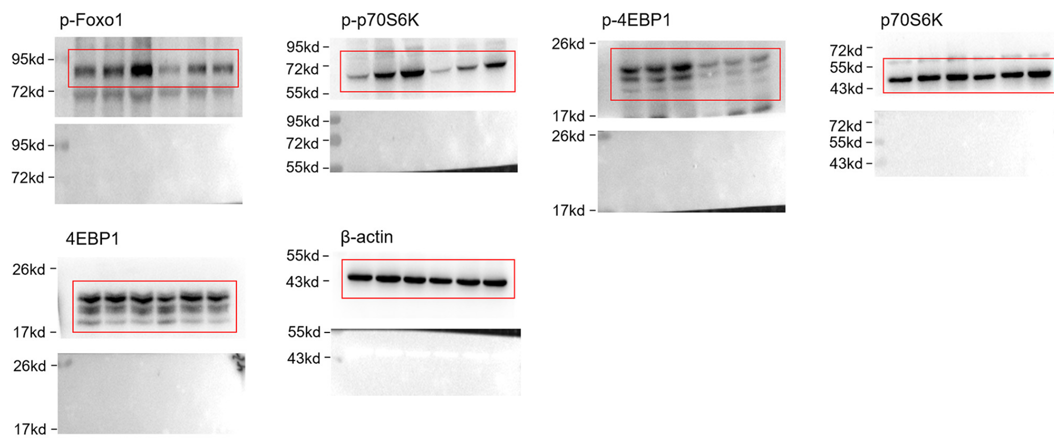

fig. S7G